PERGAMON

International Journal of Heat and Mass Transfer 43 (2000) 757–765

International Journal of HEAT and MASS TRANSFER

www.elsevier.com/locate/ijhmt

Crystal ice formation of solution and its removal phenomena at cooled horizontal solid surface Part II: onset of ice removal condition

Tetsuo Hirata[a,*], Mitsutoshi Kato[b], Koji Nagasaka[c], Masaaki Ishikawa[a]

[a] *Department of Mechanical Systems Engineering, Shinshu University, Wakasato 500, Nagano 380-8553, Japan*
[b] *Denso Co. Ltd., 1-1 Showacho, Kariya 448-8661, Japan*
[c] *Shinryo Reinetsu Co. Ltd., 2-4 Yotsuya, Shinjuku-ku, Tokyo 160-8510, Japan*

Received 24 July 1998; received in revised form 12 May 1999

Abstract

Experimental studies for crystal ice formation and its removal phenomena of ethylene glycol solution on a cooled horizontal plate have been performed. Onset condition for ice removal phenomenon is examined experimentally as well as analytically. As a cooled plate, a glass, an acrylic resin, a polyvinyl chloride, a silicone resin and the copper plates are used. It is found that the removal or unremoval of crystal ice is related to the heat flux at the cooled plate surface when the latent heat of freezing is discharged with ice formation, and that the heat flux ratio, q_2/q_1, is an important parameter of the onset condition for ice removal, where q_1 represents the heat flux from the plate surface to the cooled plate and q_2 represents the heat flux from the plate surface to the solution. It is also found that the occurrence of ice removal phenomenon is easier in the case of plastic cooling plates than that of metal ones.

Keywords: Ice formation; Ice removal phenomena; Solution; Liquid-like ice; Cold thermal energy storage

1. Introduction

In the case that ice formation occurs on a cold surface, it is well known that the ice formation rate per unit time decreases with increasing ice layer thickness due to the decrease of thermal conductance through the deposited ice layer. For a static-type cold thermal energy storage system, this characteristic may be a disadvantage since the cold thermal energy storage rate decreases with ice growth. In recent years, liquid-like ice has been utilized in the ice storage system because of its transportability using a pipe. Though a number of methods have been proposed to make ice, authors have examined a new method to make liquid-like ice continuously without the deposition of an ice layer on the cooled plate. The new method is based on the phenomenon that the crystal ice formed in the solution on the cooled plate is removed from the plate surface due to the buoyancy force acting on the crystal ice. The Part I of this paper [1] reported the crystal ice formation characteristics and the ice removal phenomenon. In the present paper, the onset condition for the ice removal phenomenon on the cooled plate is investigated experimentally as well as analytically.

* Corresponding author. Tel.: +81-26-269-5105; fax: +81-26-269-5109.
E-mail address: hirata@skip.shinshu-u.ac.jp (T. Hirata).

0017-9310/00/$ - see front matter
PII: S0017-9310(99)00181-7

Nomenclature

a	thermal diffusivity	q	heat flux
A	heat transfer area of cooled plate	q_v	heat generation per unit volume
Bi	Biot number	Q_v	dimensionless heat generation
C	solute concentration	y_1	cooled plate thickness
C_p	specific heat	y_2	thickness of heat generation layer
h	heat transfer coefficient	Y	dimensionless coordinate
L	latent heat of freezing	θ_s	dimensionless mean temperature of plate surface
m	total ice volume		
M	dimensionless total ice volume	λ	thermal conductivity
S	cohesion area of ice	ρ	density
Ste	Stefan number	τ	dimensionless time
t	time		
T_f, T_s, T_w	freezing, plate surface and plate rear surface temperatures	*Subscripts*	
		1	cooled plate
T_i	initial temperature	2	solution
$\bar{T}_s$	mean temperature of plate surface	i	ice
P	cohesion force per unit area		

2. Experiment

2.1. Experiment on ice formation and its removal

Experimental apparatus was basically the same as that reported in Part I of this paper [1]. The test section made of 15 mm thick acrylic resin plates had a dimension of $78 \times 200 \times 98$ mm^3 in inner volume. At the bottom of the test section, the test plate of 3 mm thickness was installed horizontally. The test plate was cooled with the copper plate having the dimensions of 42×193 mm^2 in heat transfer area and 3 mm thickness, which was installed on the rear surface of the test plate with an adhesive agent. Ethylene glycol solution was filled in the upper region of the test plate and the ice formation was made with cooling the rear side of the copper plate with cold brine.

As a test plate, a glass, an acrylic resin, a polyvinyl chloride, a silicone resin and copper plates, whose surfaces were smooth and were cleaned with acetone, were used. The thermal properties of those test plates are shown in Table 1. The ice formation phenomenon and the onset condition for the ice removal were examined for those test plates. The experimental ranges covered in the present experiment were $-5°C < T_w < -15°C$ for the rear surface temperature of the test plate and $C = 2$–10.0 wt% for the concentration of the ethylene glycol solution.

As reported in Part I of this paper [1], the observed ice formation phenomena are as follows. At the first stage of ice formation, the crystal ice nucleates on the plate surface and grows in the shape of thin leaf. After the growth in a certain dimension, the crystal ice is removed due to the buoyancy force acting on the ice. It was observed that the crystal ice-front grew slightly upward and did not contact with the cooled plate except the nucleation point. On the other hand, for larger cooling heat fluxes, it appeared that the ice grew in the shape of dendrite without leaving clearance on the cooled plate and was not removed, because the

Table 1
Thermal properties of cooled plates at 0°C

Plate material	Thermal conductivity λ_1 (W/m K)	Thermal diffusivity a_1 (mm^2/s)
Copper	399	118
Mercury	7.9	4.2
Glass	1.34	0.86
Silicone resin	0.21	0.115
Acrylic resin	0.21	0.12
Polyvinyl chloride	0.16	0.12
Demnum	0.148	0.0776

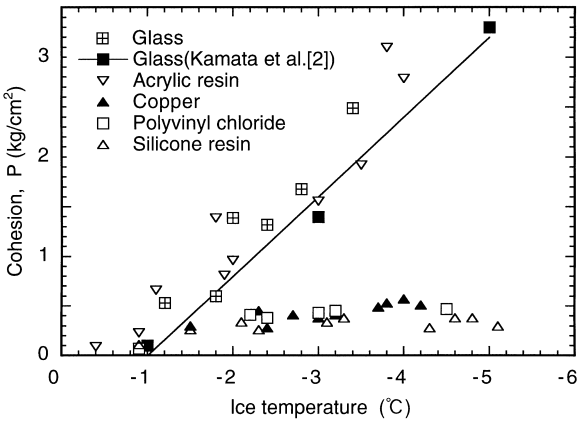

Fig. 1. Cohesion between ice and test plate.

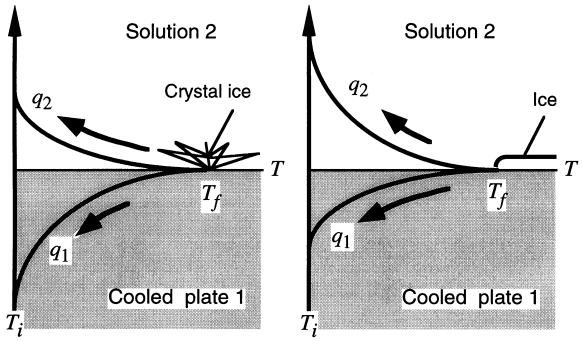

(a) $q_2 > q_1$ (b) $q_2 < q_1$

Fig. 2. Heat transfer model for latent heat of freezing.

buoyancy force acting on the ice was weaker than the cohesion force of ice in those conditions. Therefore, it is considered that the onset condition for the ice removal is related to the morphology of crystal ice growth.

2.2. Experiment on ice cohesion

For the ice removal phenomenon, the cohesion between the ice and the cooled plate is considered to be a suppression factor. The values of cohesion were measured for the test plates made of glass, acrylic resin, copper, polyvinyl chloride and silicone resin, respectively. The experimental apparatus consisted of the temperature-controlled room, a motor and a pull-guage. The experimental method was referenced from Kamata et al. [2]. The test ice was made in the copper pipe (having 26 mm inner diameter and 45 mm height) which was placed on the test plate cooled at $-15^{\circ}C$. The copper pipe filled with ice was kept in the temperature-controlled room at 0 to $-5^{\circ}C$. After a steady-state condition was reached in the ice temperature, the hooks installed on the ice and the test plate, respectively, were pulled at a constant speed with the motor-driven wire. The cohesion was measured with the pull-gauge when the ice and the test plate were taken apart.

Fig. 1 shows the results of measured cohesion for various ice temperatures. It is shown that the present data for the glass coincide satisfactorily with the result by Kamata et al. [2]. It is seen that the values of cohesion for the acrylic resin and the glass plates increase with decreasing ice temperature. On the other hand for copper, silicone and polyvinyl chloride plates, the values of cohesion show comparatively smaller values. This implies that the silicone or the polyvinyl chloride plate is preferable for the ice removal at lower plate temperatures.

3. Necessary condition on the onset of ice removal phenomenon

3.1. Heat flux condition

In the present experiment, the ice formation phenomenon occurs under the condition that the temperature distribution exists in the solution as well as in the cooled plate (see Fig. 6). As a first step toward analytical study, consider the heat transfer in the very thin layers above and below the cooled plate surface. Then, the initial temperature distributions before the ice nucleation in those layers can be assumed to be uniform. Fig. 2 shows analytical models of the crystal ice growth. At the initial conditions, the cooled plate and the solution are assumed being supercooled uniformly at the same temperatures below the freezing temperature of the solution, T_i. When the crystal ice nucleated at the plate surface, the surface temperature increases to T_f due to the discharge of latent heat of freezing. Then, the latent heat at the plate surface is conducted to the cooled plate and to the solution as q_1 and q_2, respectively. When $q_2 > q_1$, the latent heat is largely conducted to the solution as compared to that to the cooled plate and, therefore, the ice front grows apart from the plate surface, as shown in Fig. 2(a). On the other hand, when $q_2 < q_1$ the ice grows over the cooled plate without leaving clearance on the plate surface, as shown in Fig. 2(b). In this case, the buoyancy force does not act on the ice and, therefore, the ice is not removed from the surface. It is, therefore, assumed that the onset condition for the ice removal is given by

$$\frac{q_2}{q_1} > 1 \tag{1}$$

To obtain the values of q_1 and q_2, it is assumed that (1) the cooled plate and the solution are semi-infinite bodies which are kept initially at the supercooled tem-

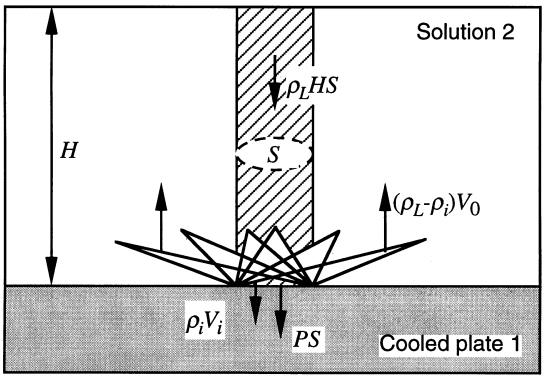

Fig. 3. Force balance at cooled plate surface.

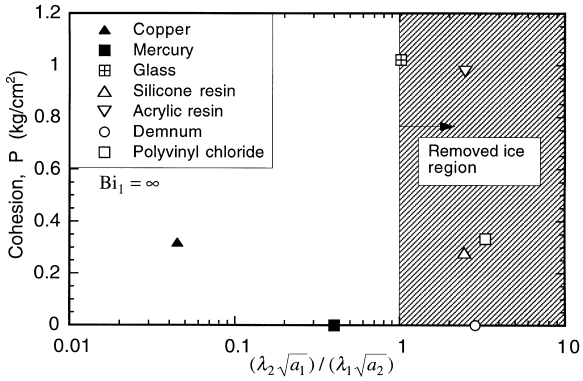

Fig. 4. Ice removal condition on cooled plate.

perature ($T = T_i$), and that (2) the surface temperature of the cooled plate is kept at the freezing temperature ($T_s = T_f$) for $t > 0$ after the ice nucleation. It should be noted that the assumption (1) is available for a short lapse of time after the ice nucleation, since a semi-infinite body is assumed for the very thin layers above and below the cooled plate surface. Then, the temperature profile within the cooled plate is given by the solution for a heat conduction problem in a semi-infinite body [3] as

$$T_1(t,y) = (T_f - T_i)\mathrm{erfc}\frac{y}{2\sqrt{a_1 t}} + T_i \tag{2}$$

The Fourier's formula of heat conduction gives

$$q_1 = -\lambda_1 \left.\frac{\partial T_1}{\partial y}\right|_{y=0} \tag{3}$$

Substituting Eq. (2) into Eq. (3) yields the heat flux conducted into the cooled plate as

$$q_1(t,0) = (T_f - T_i)\frac{\lambda_1}{\sqrt{\pi a_1 t}} \tag{4}$$

The value of q_2 is also obtained in the same manner and the heat flux ratio at the plate surface is given by

$$\frac{q_2}{q_1} = \frac{\lambda_2}{\lambda_1}\sqrt{\frac{a_1}{a_2}} \tag{5}$$

The onset condition is, therefore, given by Eqs. (1) and (5).

It should be noted that the onset condition derived above is obtained under the assumption that the initial temperature distributions within the solution and the cooled plate are uniform. This means that the value of q_2/q_1 estimated is larger than the value given by the actual temperature distributions (see Fig. 6). This implies that the ice removal phenomenon never occurs when the onset condition given above is not satisfied, and this is a necessary condition for the onset of ice removal phenomenon. It should be emphasized here that the onset value is obtained only from the thermal properties shown in Eq. (5).

3.2. Force balance condition

Fig. 3 shows the forces acting on the crystal ice. From Fig. 3, the condition that is necessary for the ice removal is given by

$$(\rho_L - \rho_i)V_o > \rho_L HS + \rho_i V_i + PS \tag{6}$$

where S is the cohesion area of the crystal ice on the cooled plate, V_i and V_o are the ice volumes inside and outside regions of the area S, respectively. In the preliminary experiment, it was found that the effect of solution head, H, on the ice removal phenomenon was negligibly small for the condition of $150 < H < 900$ mm. On the assumption that the cohesion area was negligibly small as compared to the dimension of the crystal ice, Eq. (6) is reduced to

$$(\rho_L - \rho_i)V > PS \tag{7}$$

where V $(= V_i + V_o)$ is the volume of the crystal ice. From Eq. (7), it is seen that the buoyancy force must be larger than the cohesion force, PS, for the occurrence of the ice removal phenomenon.

3.3. Comparison with experiment

In Fig. 4, the result of ice removal experiment for 4.6 wt% ethylene glycol solution is shown in the coordinate system of the ice cohesion, P, versus the heat flux ratio given by Eq. (5). The values of ice cohesion are used at -2°C of ice temperature and are estimated as zero for the cooled liquids of mercury and Demnum (fluoric oil). In Fig. 4, the open circle, square and triangle denote the results of removed ice, and the solid square and triangle denote the results of unremoved ice. Although the initial temperatures of the solution

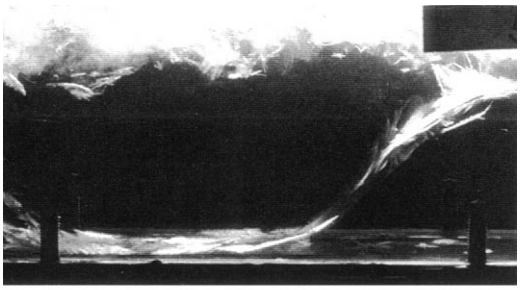

(a) C=2wt%, T_w=-13.5℃.

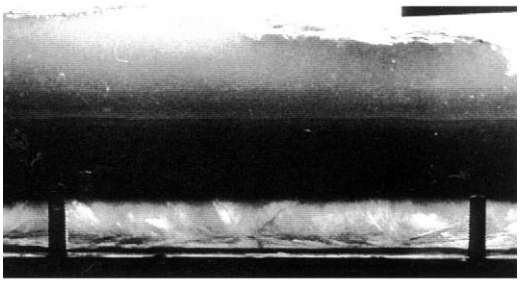

(b) C=2wt%, T_w=-20.7℃.

Fig. 5. Ice removal and unremoval phenomena.

and the cooled plate were not uniform in the experiment, it is considered that the experimental results can be compared with the analytical ones for comparatively higher cooling temperatures (see Section 4.1). It is seen that the experimental results coincide with the analytical results given by Eqs. (1) and (5). For the glass plate, it was observed that the ice removal occurred but sometimes the ice became unremoved during the experiment. This phenomenon can be realized from the fact that the thermal properties of glass is just at the onset condition of $q_2/q_1 = 1$, as shown in Fig. 4. In Fig. 4, it is also shown that the ice cohesion does not affect the ice removal condition. This implies that the cohesion area on the cooled plate, S, is extremely small because the crystal ice-front grows apart from the plate surface. As a result, the effect of the cohesion force, PS, is small enough for the ice removal phenomenon and does not appear apparently in the present experimental conditions. In the following discussion, therefore, the effect of ice cohesion will be neglected.

It should be noted that the ice removal condition shown in Fig. 4 is obtained from the analytical models shown in Fig. 2. That is, the initial temperature distributions within the cooled plate and the solution are assumed as uniform. Therefore, the applicable range of the analytical models shown in Fig. 2 exists. However,

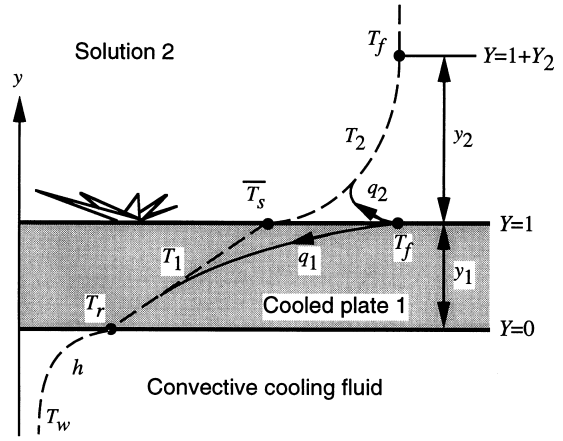

Fig. 6. Analytical model.

it can be concluded that the onset condition is related to the heat flux ratio at the plate surface, q_2/q_1.

4. Onset of ice removal phenomenon for actual temperature distribution

4.1. Ice removal and unremoval phenomena

In the experiment, it was observed that the ice removal did not occur for lower temperatures even if the value of q_2/q_1 was in the ice removal condition. Fig. 5 shows the results of ice removal and unremoval phenomena observed for 2 wt% ethylene glycol solution. For comparatively higher cooling temperatures, the ice removal occurs, as shown in Fig. 5(a). It was observed that the joining of ice crystals occurred at many locations on the cooled plate, and the ice grew in the shape of sheet having almost the same dimension as that of the cooled plate. After the removal of the ice sheet, several ice crystals nucleated again on the plate surface and the same phenomena occurred repeatedly. For lower cooling temperatures, it was observed that a number of ice crystals nucleated on the test plate. As time elapsed, the ice grew as a dendritic ice layer and the ice removal did not occur, as shown in Fig. 5(b). In this case, it is guessed that the secondary ice growth occurs at the clearance between the ice and the plate surface and the clearance is partly filled with ice. Consequently, the buoyancy force acting on the ice sheet becomes weak to peel off the ice from the cooled plate. From these observations, it is concluded that the value of cooling heat flux through the plate is an important factor for the ice removal condition. This means that the initial temperature distribution within the cooling plate affects the ice removal phenomenon, and that the onset condition should be

derived for the case of non-uniform initial temperature.

4.2. Onset condition for ice removal phenomenon

In this section, the onset condition is examined for actual temperature profiles. Fig. 6 shows temperature profiles before and after the ice nucleation by a dashed and a solid line, respectively. It is assumed that the surface temperature of the cooled plate before the ice nucleation is supercooled at $\bar{T}_s$ and that the rear surface of the plate is cooled by a convective heat transfer. When the ice nucleation occurs at the surface of the cooled plate, it is assumed that the surface temperature rises at the freezing temperature of the solution, T_f, due to the discharge of latent heat of freezing. Then, the surface heat fluxes to the cooled plate, q_1, and to the solution, q_2, in the transient process can be estimated by a numerical calculation.

4.2.1. Mean temperature profiles

To obtain the mean temperature profiles shown in Fig. 6 as a dashed line, the dimensionless parameters are defined as

$$a_2^* = \frac{a_2}{a_1}, \quad Bi_1 = \frac{hy_1}{\lambda_1} \quad M = \frac{m}{Ay_1},$$

$$Ste_1 = \frac{C_{p_1}(T_f - T_w)}{L}, \quad Q_v = \frac{1}{\lambda_2^*}\frac{q_v y_1^2}{\lambda_1(T_f - T_w)},$$

$$Y = \frac{y}{y_1}, \quad \theta = \frac{(T - T_w)}{(T_f - T_w)}, \quad \theta_s = \frac{(\bar{T}_s - T_w)}{(T_f - T_w)},$$

$$\lambda_2^* = \frac{\lambda_2}{\lambda_1}, \quad \rho_i^* = \frac{\rho_i}{\rho_1}, \quad \tau = \frac{a_1}{y_1^2}t \tag{8}$$

The heat conduction equation in the cooled plate and its boundary conditions are given by

$$\frac{\partial^2\theta_1}{\partial Y^2} = 0 \tag{9}$$

$$Y = 0: \quad \theta_1 = \theta_r$$

$$Y = 1: \quad \theta_1 = \theta_s \tag{10}$$

The temperature profile within the cooled plate is obtained from Eqs. (9) and (10).

$$\theta_1 = \left(\frac{Bi_1}{1 + Bi_1}Y + \frac{1}{1 + Bi_1}\right)\theta_s \tag{11}$$

where the heat balance equation at $Y = 0$ given by the following equation was used.

$$\theta_r = \frac{1}{1 + Bi_1}\theta_s \tag{12}$$

On the other hand, the heat conduction equation in the solution is given by the assumption that the discharged latent heat into the solution is considered as heat generation within the solution.

$$\frac{\partial^2\theta_2}{\partial Y^2} + Q_v = 0 \tag{13}$$

where Q_v represents the dimensionless heat generation rate per unit of volume. The boundary conditions for Eq. (13) are given by

$$Y = 1: \quad \theta_2 = \theta_s$$

$$Y = 1 + Y_2: \quad \theta_2 = 1 \tag{14}$$

The temperature profile within the solution is obtained from Eqs. (13) and (14).

$$\theta_2 = -\frac{Q_v}{2}Y^2 + \left[\frac{Q_v}{2}(Y_2 + 2) + \frac{1 - \theta_s}{Y_2}\right]Y - \frac{Q_v}{2}(Y_2 + 1) - \frac{1 - \theta_s}{Y_2} + \theta_s \tag{15}$$

As the heat generation rate is equal to the discharged latent heat by freezing, the following equation is given:

$$Ay_2 q_v = \rho_i L\frac{dm}{dt} \tag{16}$$

where A is the heat transfer area of the cooled plate and y_2 is the thickness of the heat generation layer in the solution. In a steady-state condition, the discharged latent heat of freezing is equal to the conduction heat through the cooled plate.

$$\rho_i L\frac{dm}{dt} = A\lambda_1\frac{\bar{T}_s - T_r}{y_1} \tag{17}$$

The dimensionless heat generation rate is given by substituting Eq. (17) into Eq. (16).

$$Q_v = \frac{\theta_s}{\lambda_2^* Y_2}\left(\frac{Bi_1}{1 + Bi_1}\right) \tag{18}$$

The heat balance equation at the plate surface is given by

$$\left.\frac{\partial\theta_1}{\partial Y}\right|_{Y=1} = \lambda_2^*\left.\frac{\partial\theta_2}{\partial Y}\right|_{Y=1} \tag{19}$$

Substituting Eqs. (11) and (15) into Eq. (19) and using the relation of (18) yield the dimensionless thickness of the heat generation layer.

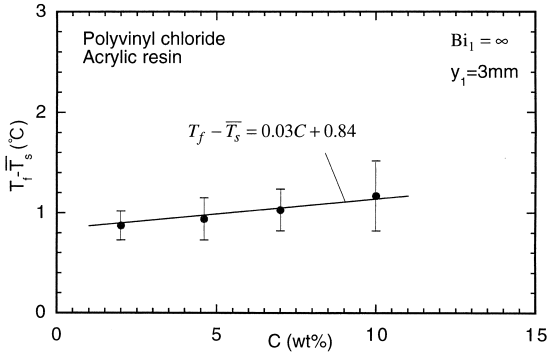

Fig. 7. Mean surface temperature of cooled plate surface.

$$Y_2 = \frac{2\lambda_2^*(1-\theta_s)}{\theta_s}\frac{(1+Bi_1)}{Bi_1} \tag{20}$$

If the value of θ_s was known, the temperature profile within the solution could be calculated by substituting Eqs. (18) and (20) into Eq. (15).

Fig. 7 shows the mean surface temperature of the cooled plate obtained for the polyvinyl chloride and the acrylic resin plates. The empirical equation for θ_s is given by

$$\theta_s = 1 - \frac{0.03C + 0.84}{T_f - T_w} \tag{21}$$

Fig. 8 shows the analytical result for the thickness of the heat generation layer in the solution, where y_2 is represented in the dimension of mm. It is seen that the value of y_2 increases with solute concentration. This result coincides with the observation that the crystal ice-front grows apart from the plate surface for higher concentrations as compared to that for lower ones. It is also shown that the value of y_2 decreases for lower cooling temperatures, T_w. This implies that the crystal ice grows closely on the plate surface for larger cooling heat fluxes, which results in weaker buoyancy force because of less clearance between the crystal ice and

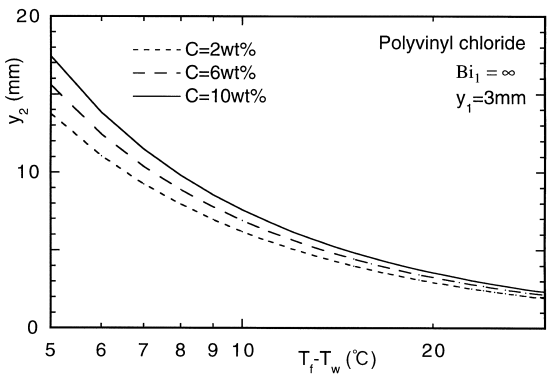

Fig. 8. Thickness of latent heat discharged layer.

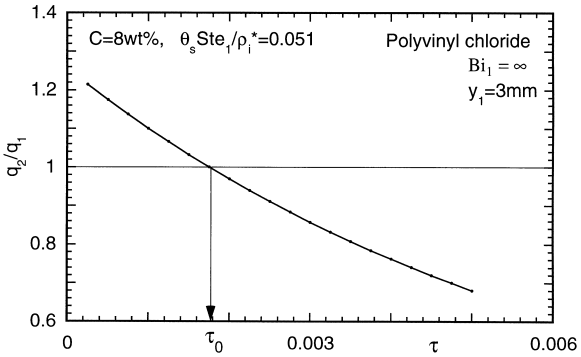

Fig. 9. Change of heat flux ratio with time.

the plate surface. This result explains the phenomenon that the ice becomes unremoved for larger heat fluxes, as shown in Fig. 5.

4.2.2. Calculation for ice removal condition

Suppose that the initial temperature profiles within the cooled plate and the solution are given by Eqs. (11) and (15), respectively, and that the plate surface temperature rises at $T = T_f$ with ice nucleation for $t > 0$. Then, the ratio of surface heat flux q_2/q_1 in the transient process can be obtained by a numerical calculation. The heat conduction equations in the transient process for the cooled plate and for the solution are, respectively, given by

$$\frac{\partial\theta_1}{\partial\tau} = \frac{\partial^2\theta_1}{\partial Y^2} \tag{22}$$

$$\frac{\partial\theta_2}{\partial\tau} = a_2^*\frac{\partial^2\theta_2}{\partial Y^2} \tag{23}$$

The boundary conditions for Eqs. (22) and (23) are given by the following initial conditions:

$$\theta_1(0,Y) = \theta_1$$

$$\theta_2(0,Y) = \theta_2$$

$$\theta_1(\tau,1) = \theta_2(\tau,1) = 1 \tag{24}$$

The values of θ_1 and θ_2 in the transient process are obtained from Eqs. (22)–(24). Then, the heat flux ratio at the plate surface is calculated by

$$\frac{q_2(\tau)}{q_1(\tau)} = \lambda_2^*\frac{\partial\theta_2}{\partial Y}\bigg|_{Y=1}\Big/\frac{\partial\theta_1}{\partial Y}\bigg|_{Y=1} \tag{25}$$

Fig. 9 shows the change of heat flux ratio versus the dimensionless time after the ice nucleation. During the early stage of the transient process, it is shown that the latent heat is discharged largely into the solution, $q_2/$

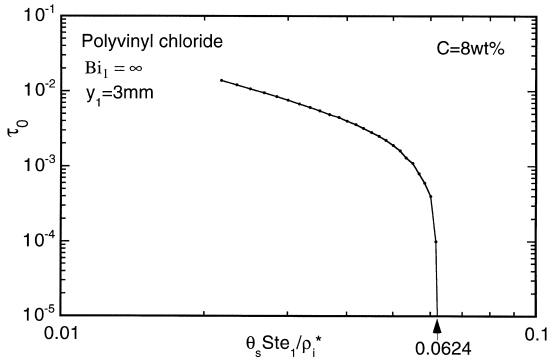

Fig. 10. Change of τ_o with dimensionless cooling temperature.

$q_1 > 1$. However, the value of heat flux ratio changes into $q_2/q_1 < 1$ at $\tau = 0.0018$. Here, the value of τ at $q_2/q_1 = 1$ is defined by τ_o. Then, it is noted that the crystal ice formed on the cooled plate is removable for $\tau < \tau_o$ and unremovable for $\tau > \tau_o$.

The ice formation rate given by Eq. (17) is rewritten into a dimensionless form as

$$\frac{1 + Bi_1}{Bi_1}\frac{\mathrm{d}M}{\mathrm{d}\tau} = \frac{\theta_s Ste_1}{\rho_i^*} \tag{26}$$

In Fig. 10, the calculated result of τ_o is shown against the value on the right-hand side in Eq. (26), which represents a dimensionless cooling temperature. It is shown that the value of τ_o decreases for lower cooling temperatures and reaches to $\tau_o = 0$ at $\theta_s Ste_1/\rho_i^* = 0.0624$ under the conditions shown in Fig. 10. This means that the ice removal condition of $q_2/q_1 > 1$ is never satisfied for $\theta_s Ste_1/\rho_i^* > 0.0624$. Therefore, the value of $\theta_s Ste_1/\rho_i^*$ at $\tau_o = 0$ is the onset condition for the ice removal phenomenon.

4.3. Comparison with experimental results

Fig. 11 shows the comparison with the experimental

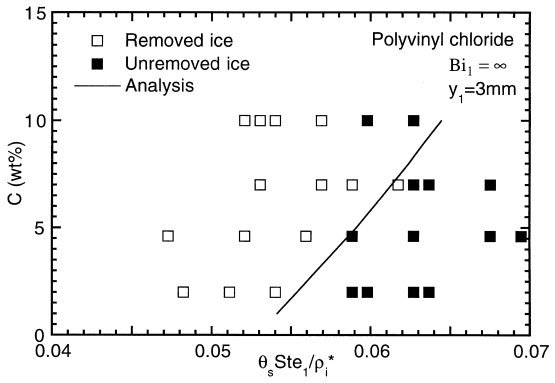

Fig. 11. Comparison of ice removal condition.

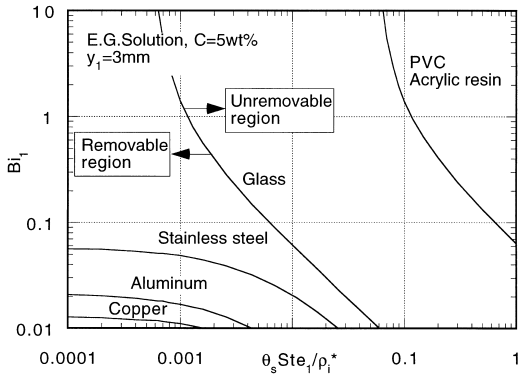

Fig. 12. Onset condition for ice removal phenomenon.

results for various concentrations of ethylene glycol solution. It is shown that the crystal ice becomes unremoved for lower cooling temperatures (larger values of $\theta_s Ste_1/\rho_i^*$), as observed in Fig. 5. In Fig. 11, it should be emphasized that the crystal ice is never removed in the right-hand side region of the analysis line, as discussed in Section 4.2.2. Taken into account that the experiment under a condition close to the onset can be affected by a small disturbance of the controlled temperatures, it can be noted that the analytical result coincides with the experiment. It is also shown in Fig. 11 that the ice removal phenomenon occurs easily for higher solute concentrations. This result is explained from the result shown in Fig. 8, which implies that the crystal ice-front can grow apart from the plate surface for lower cooling temperatures because of increasing thickness of the heat generation layer with solute concentration.

Fig. 12 shows the onset conditions for various plate materials. The ordinate is a Biot number that represents the cooling heat transfer coefficient on the rear surface of the test plate. It should be noted again that the right-hand side of each analysis line is unremovable region. It is shown that the polyvinyl chloride and the acrylic resin plates are removable materials for larger Biot numbers. However, for the metal plates such as stainless steel, aluminum and copper, the crystal ice can be removed only for very small Biot numbers and very high cooling temperatures. For those materials, it is guessed that the continuous ice removal may be difficult because the precise temperature control for the cooled plate will be needed.

5. Conclusions

The onset of ice removal condition for the ethylene glycol solution on the cooled plate with the thickness of $y_1 = 3$ mm is examined experimentally as well as analytically. The following conclusions can be drawn:

1. The onset condition for the ice removal is related to a heat flux ratio, q_2/q_1, at the cooled plate surface. The crystal ice becomes unremoved for larger cooling heat fluxes, that is, for lower cooling temperatures.
2. For larger Biot numbers, the onset condition for the ice removal is related to the thermal properties of the cooled plate and of the solution, and is given by Eqs. (1) and (5).
3. The map for the onset condition is given in Fig. 12. For the occurrence of the ice removal phenomenon, plastic plates are preferable to metal ones.

Acknowledgements

This work was supported by the 'Research for the future' Program of the Japan Society for the Promotion of Science, JSPS-RFTF97P01003.

References

[1] T. Hirata, K. Nagasaka, M. Ishikawa, Crystal ice formation of solution and its removal phenomena at cooled horizontal solid surface Part I: ice removal phenomena, Int. J. Heat and Mass Transfer 43 (2000) 333–339.
[2] Y. Kamata, Y. Mizuno, K. Horiguchi, M. Yoshida, Ice adhesion near the melting point, in: Y. Lee, W. Hallett (Eds.), Proceedings of the Fifth International Symposium on Thermal Engineering and Science for Cold Regions, Ottawa, 1996, pp. 453–458.
[3] H.S. Carslaw, J.C. Jaeger, Conduction of Heat in Solids, Oxford University Press, New York, 1988.